ELSEVIER

Available online at www.sciencedirect.com

ScienceDirect

Journal of Nuclear Materials 375 (2008) 340–346

journal of nuclear materials

www.elsevier.com/locate/jnucmat

Transmission electron microscopy investigation of irradiated U–7 wt%Mo dispersion fuel

S. Van den Berghe *, W. Van Renterghem, A. Leenaers

SCK·CEN, Nuclear Materials Science Institute, Boeretang 200, 2400 Mol, Belgium

Received 13 August 2007; accepted 8 December 2007

Abstract

The microstructural evolution of atomised U–7 wt%Mo alloy fuel under irradiation was investigated by transmission electron microscopy on material from the experimental fuel plates used in the FUTURE irradiation. The interaction layer that forms between the U(Mo) particles and the Al matrix is assumed to become amorphous under irradiation and as such cannot retain the fission gas in stable bubbles. As a consequence, gas filled voids are generated between the interaction layer and the matrix, causing the fuel plate to pillow and finally fail. The present analysis confirms the assumption that the U(Mo)–Al interaction layer is completely amorphous after irradiation. The Al matrix and the individual U(Mo) particles, with their cellular substructure, have retained their crystallinity. It was furthermore observed that the fission gas generated in the U(Mo) particles has formed a bubble superlattice, which is coherent with the U(Mo) lattice. Bubbles of roughly 1–2 nm size have formed a 3-dimensional lattice with a lattice spacing of 6–7 nm.

1. Introduction

Since the 1970s, much effort has been devoted to replacing the high-enriched, low-density UAl_x-based dispersion fuel, which is generally used in research reactors, with high-density, low-enriched (<20% $^{235}U/U_{tot}$) alternatives. This search is driven by the attempt to reduce the civil use of high-enriched materials because of proliferation risks and terrorist threats. American initiatives, such as the Global Threat Reduction Initiative (GTRI) and the Reduced Enrichment for Research and Test Reactors (RERTR) program, as well as French R&D programs directed towards fuel development for the Jules Horowitz reactor that is currently under construction, have particularly triggered the development of reliable low-enriched fuel types for these reactors, which can replace the high-enriched ones without loss of performance. Most success has been obtained with U_3Si_2 fuel, which is currently used in many research reactors in the world [1]. However, efforts to search for a better replacement have continued, particularly in view of the undesirable characteristics of U_3Si_2 with respect to reprocessing [2] and for those reactors that cannot convert to U_3Si_2-based fuel without loss in performance. Most of these efforts are currently directed towards the higher density U–Mo alloy fuel (7–10 wt% Mo).

Pure U metal would in principle be a straightforward high-density fuel material, but only the high-temperature, isotropic uranium γ-phase behaves stable under irradiation, while its room temperature α-phase structure shows important swelling. A transformation of γ to α (through the β phase) cannot be suppressed by quenching the pure high-temperature U-γ phase, but the temperature range over which the α, β, and γ phase are stable can be altered by alloying the material [3]. Molybdenum exhibits a high degree of solid solubility in γ-uranium. If cooled slowly or if the alloy contains less than 7 at.% Mo, the equilibrium state of U(Mo) alloys below 560 °C is a mixture of α-U and a γ′-phase (U_2Mo), while a γ-U/Mo solid solution is found at high-temperature [3]. By quenching the U(Mo) alloy from the γ-phase, a metastable γ-state will be retained at

---

* Corresponding author. Tel.: +32 14 333064; fax: +32 14 321216.
E-mail address: svdbergh@sckcen.be (S. Van den Berghe).

0022-3115/$ - see front matter © 2008 Elsevier B.V. All rights reserved.
doi:10.1016/j.jnucmat.2007.12.006

room temperature. These γ-U(Mo) alloys are considered to be one of the most promising uranium alloys to be used as dispersion fuels [4].

The French Program for U(Mo) fuel, launched in 1999, made important contributions to the development of U(Mo) dispersion fuel [5]. They performed several irradiations of full-sized experimental plates with low-enriched uranium ($^{235}U/U_{tot} = 19.8\%$) and high uranium loading up to 8.5 g/cm^3. In one such experiment, fuel plates containing U-7 wt% Mo atomised powder were irradiated in the FUTURE irradiation rig of the BR2 reactor at the Belgian nuclear research centre SCK·CEN. At a burn-up of approximately 33% ^{235}U (6.5% FIMA or 1.41×10^{21} fissions/cm^3 meat), the fuel plates showed important deformations and the irradiation was stopped. The plates were submitted to detailed post-irradiation examinations (PIE) at the Laboratory for High and Medium Activity (LHMA) at SCK·CEN. The results of these examinations were reported in [6,7].

The FUTURE experiment is ever since regarded as the definitive proof that the classical atomised U(Mo) dispersion fuel is not stable under irradiation after all, at least under the conditions required for normal operation of plate-type fuel. The main cause for the instability was identified to be the irradiation behaviour of the U(Mo)–Al interaction phase which is formed between the U(Mo) particles and the pure aluminium matrix during irradiation [6,7]. The phase showed poor fission gas retention, causing large pores to develop between the interaction layer and the matrix aluminium, which eventually led to gross swelling and pillowing of the fuel plates.

This paper studies the microstructural aspects of the irradiated fuel of the FUTURE-experiment in more detail using transmission electron microscopy (TEM), in an attempt to understand the nature of the interaction phase and the fission gas behaviour in the atomised U(Mo) fuel.

2. Experimental

A sample of irradiated U(Mo) fuel was taken adjacent to the specimen used in the post-irradiation examinations of the FUTURE irradiation reported in [6]. The cross-sectional sample was polished down to a thickness of around 100 µm, after which it was cut into small fragments. One fragment was glued on a golden grid with an aperture of 1 mm. Final thinning of the sample was done with twin jet electropolishing using an electrolyte composed of 5% perchloric acid in methanol at −45 °C applying a voltage of 20 V [8].

Because of the heterogeneously dispersed phases present in the sample, it was necessary to get an overview on the location of the holes in the sample with respect to the U(Mo) particles, the matrix aluminium, the cladding aluminium and the interaction phase. An image was obtained by scanning electron microscopy (SEM) of the sample to locate the appropriate areas in the sample for TEM investigation (Fig. 1).

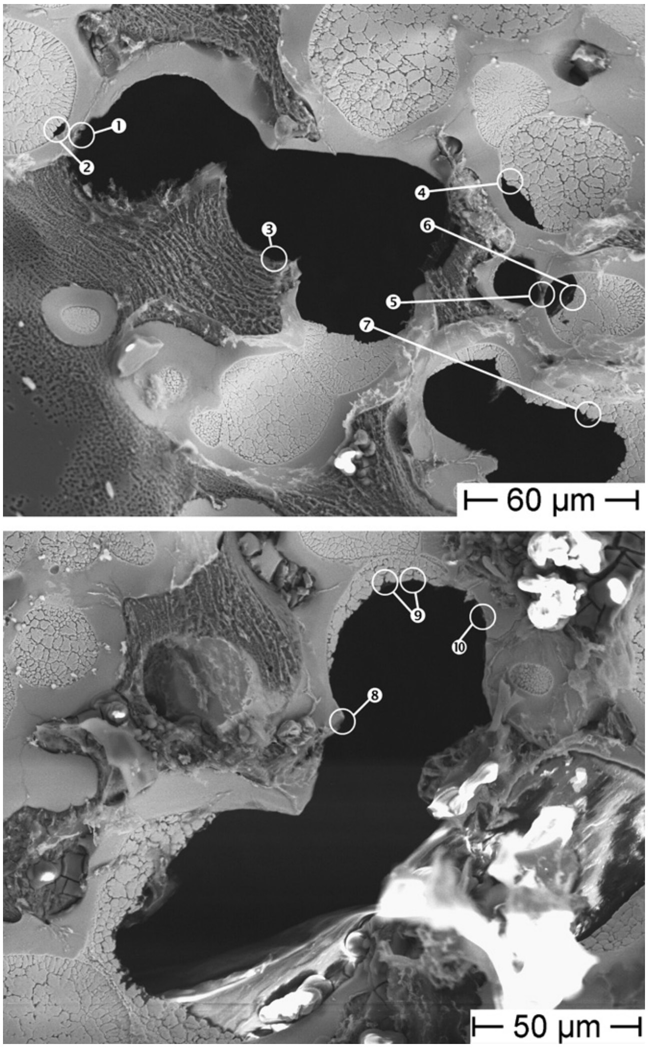

Fig. 1. Scanning electron micrographs of the holes in the irradiated sample produced by the twin jet electrochemical polishing. The numbered areas indicate the regions in which the TEM analyses were performed and are referenced in the text and figure captions.

SEM was performed on a fully shielded Jeol JSM-6310 microscope with backscattered and secondary electron detectors. TEM was done using a JEOL JEM-3010 microscope operating at 300 kV. Conventional bright field and dark field imaging was applied, along with electron diffraction patterns for phase identification.

3. Results

Only a very small area adjacent to the hole is transparent for the electrons, but as seen from the scanning electron micrograph shown in Fig. 1, the various phases present in the sample extend to the hole and are accessible for TEM investigation at various locations. One can clearly observe the cellular substructure of the atomised U(Mo) particles, which is accentuated by the electrochemical polishing procedure that preferentially attacked the cell boundaries. Since the chemical agent used in the electropolishing is aimed at U alloys, it is remarked that it has attacked aluminium in a very different way, which results in the observed aspect of the Al phase in the SEM image. The areas where TEM imaging and analysis were performed are indicated by the circles in Fig. 1 and include

- the interaction phase that has formed between the U(Mo) fuel and the Al matrix (locations 1, 5, 8 and 10),
- the U(Mo) fuel particles with attention for the cellular structure and the phase in between the cells (locations 2, 4, 6, 7 and 9),
- the pure Al matrix (location 3).

Not all investigated locations are described in detail in this paper, but the recorded aspects of the fuel were shown to be general and not related to a particular location on the sample.

Analysis of the interaction phase between the atomised particles and the matrix shows that it has a completely featureless character (Fig. 2(a)) and is fully amorphous, as seen by its diffraction pattern (Fig. 2(b)). The interaction phase was studied at various locations (Fig. 1), but the amorphous phase was found everywhere. Measuring the average nearest neighbour distance based on the ring observed in the diffraction pattern, we obtain (0.239 ± 0.004) nm as an average and spread of five individual measurements at different locations on the specimen.

A typical dark-field image of a U(Mo) grain and its corresponding diffraction pattern are shown in Fig. 3. The white circle in Fig. 3(a) indicates the area selected for the diffraction pattern. Although the U(Mo) phase is very clearly crystalline and has a single orientation, as seen from the diffraction pattern, the dark-field images contain a lot of grainy contrast. Part of this can be explained by the probably large defect concentration in the U(Mo) grains. However, the diffraction pattern (Fig. 3(c)) also shows reflection rings belonging to the UO_2 structure (cubic, $Fm\text{-}\bar{3}m$, $a_0 = 0.5467$ Å) in addition to the sharp reflections of the γ-U based structure of the U(Mo) phase (γ-U structure: cubic, $Im\text{-}\bar{3}m$, $a_0 = 0.3481$ Å, for U(Mo): $a_0 = 0.34808\text{–}0.000314 \times$ at.%Mo [9]). Since it is known from previous observations that no oxide is present in the fuel [6], this indicates that the material has oxidised by exposure to the electrolyte and the open atmosphere, which is known to occur for this type of material.

Dark-field images were recorded (Fig. 3(a) and (b)) using two different parts of the diffraction pattern as shown by the white circles on the pattern that approximately indicate the used position of the microscope objective aperture. The images recorded using part of the reflection ring belonging to the UO_2 structure only (Fig. 3(b)) reveal that very small oxide particles have formed in the material, as expected from an oxidised surface. For the dark-field image in Fig. 3(a), the (1 1 0) reflection of $\gamma\text{-}U(Mo)$ was selected. Because of the size of the selecting aperture, also part of the oxide ring contributes to the image. This contribution is mainly visible on the right part of the image, at the edge of the specimen, where mainly small grains can be recognized. On the left side, a more equal intensity can be observed which shows the U(Mo) phase. The contrast differences in that area are again due to small oxide grains formed on the surface. Some preferential orientation of the UO_2 particles with respect to the U(Mo) structure is clearly observed in the diffraction pattern as the diffraction rings show intensity maxima close to the position of the γ-U(Mo) reflections.

When observed more in detail and at higher magnification in bright field, the U(Mo) cells show a lattice of regularly spaced bubbles or voids. This lattice is particularly well visible at slightly under-focus conditions (Fig. 4(a)). The bubbles or voids have a size of around 2 nm and a spacing of roughly 6–7 nm. The orientation of the superlattice is coherent with the U(Mo) lattice orientation, which was checked by observation of the superstructure reflection

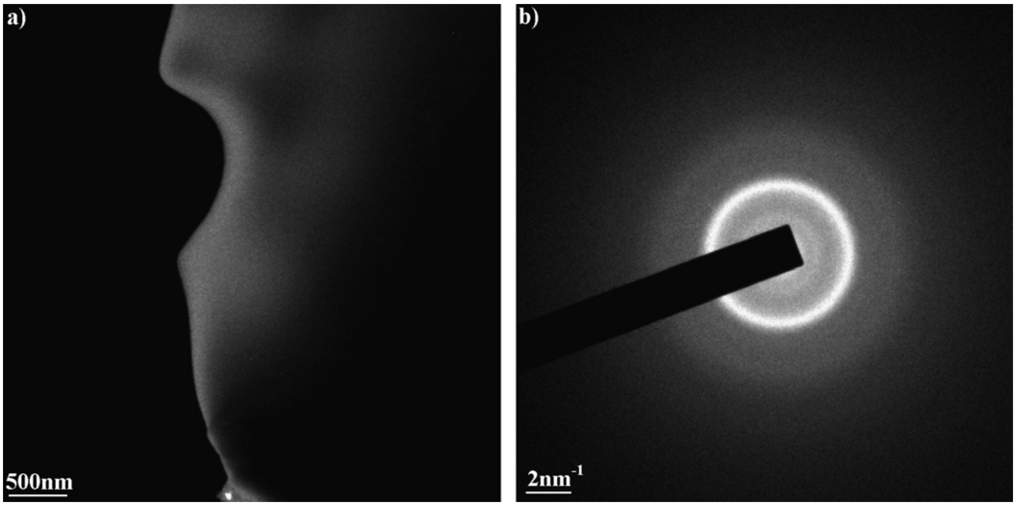

Fig. 2. (a) Dark-field image of the interaction layer with (b) the diffraction pattern, recorded at position 8 as indicated in Fig. 1, demonstrating its fully amorphous character.

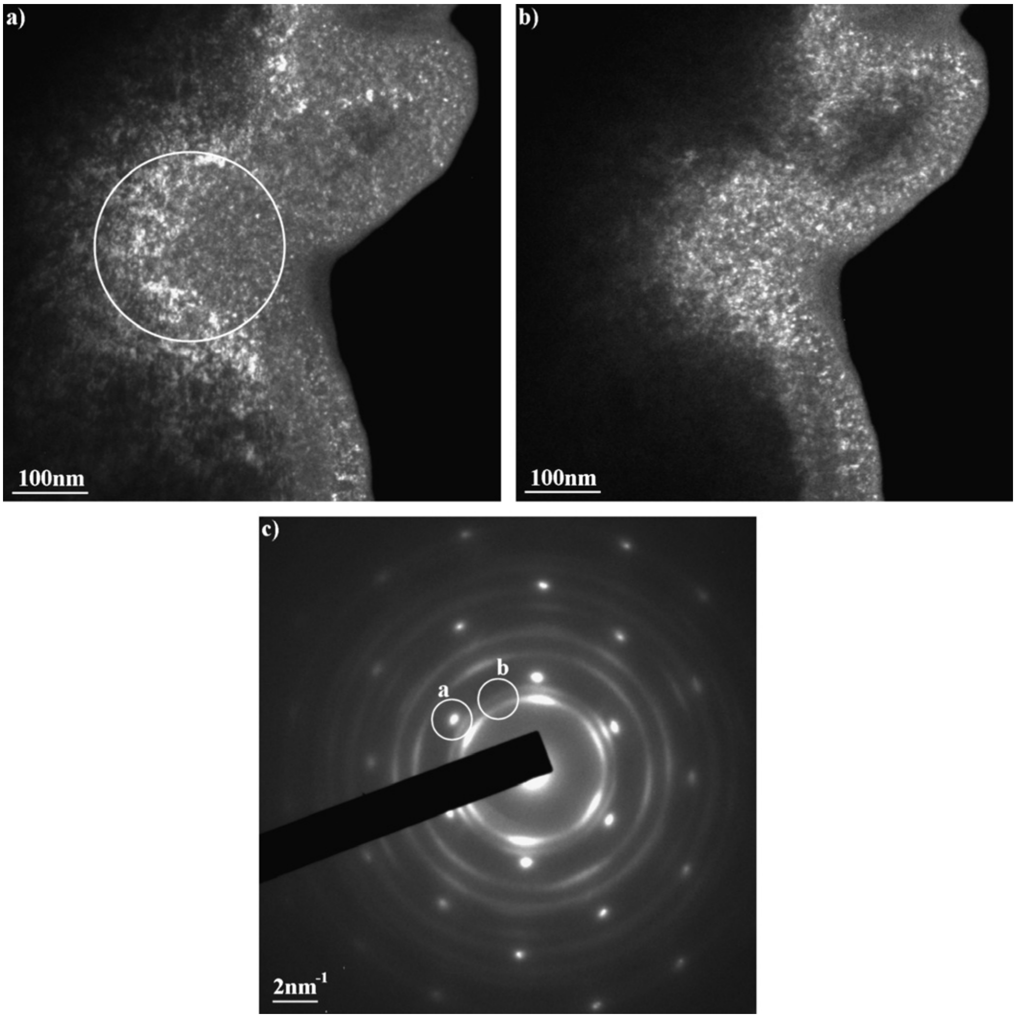

Fig. 3. Dark-field images and the diffraction pattern generated in the area indicated by the white circle of a transparent region in the U(Mo) fuel at position 6 as indicated in Fig. 1, taken using (a) the $(\bar{1}\,1\,0)$ U(Mo) reflection from the [1 1 1] zone and (b) with part of the UO2 diffraction rings from the {1 1 1} and {2 0 0} planes as indicated by the white circles in the diffraction pattern in (c).

satellites close to the U(Mo) reflections in the diffraction pattern (see inset of Fig. 4(b)). It was verified that the locations of the superstructure spots indeed correspond with a bubble spacing of 6–7 nm and their orientation corresponds with the orientation of the rows of bubbles in the bright-field image.

In between the U(Mo) cells, a uranium phase with slightly lower Mo content is located, as was already shown and discussed in [6]. The dark-field image (Fig. 5(a)) shows a featureless structure apart from some small particles. The diffraction pattern recorded at this location (Fig. 5(b)) shows a completely amorphous picture apart from a slightly higher intensity within the white circle, which is difficult to see on the photograph but shows up in digital processing. The location of the increased intensity corresponds with an interplanar distance of about 0.32 nm, which is larger than the largest interplanar distance of the γ-U(Mo) structure, but which can be related to the (1 1 1) planes of UO_2. Therefore, it can be assumed that the small particles in the dark-field image are again oxide particles, while the phase in between the U(Mo) cells is completely amorphous. However, the cell boundaries have been extensively attacked by the electrolyte, as was already remarked in the SEM observations, which could influence the results.

The pure Al matrix has retained its crystal structure and, besides the formation of a large concentration of irradiation defects, it does not show any particularities. A more detailed analysis of the Al phase was not possible in this specimen because the polishing procedure is not adapted.

4. Discussion

Observations of gross swelling of atomised U(Mo)-based, flat dispersion fuel plates have been linked to the physical properties of the interaction phase formed in-pile between the U(Mo) particles and the Al matrix [10]. The most likely explanation was given by Hofman et al. [11–13] who suggest that the phase amorphises under irradiation because of the high energy fission fragments producing damage to the crystal lattice. Such amorphisation is also

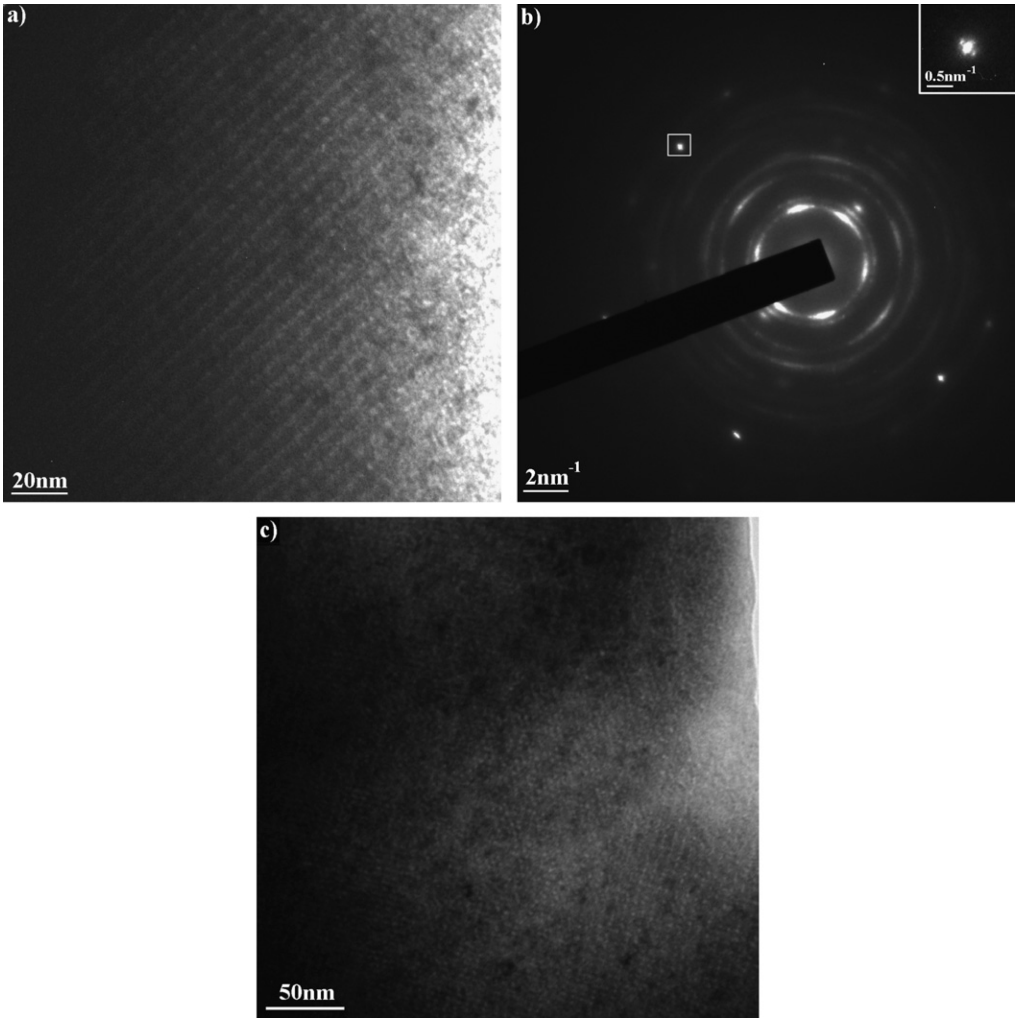

Fig. 4. (a) Bright-field image of the bubble superlattice found in the U(Mo) particles, recorded at position 7 as indicated in Fig. 1. This image was taken at slightly underfocus conditions to reveal the bubble structure more clearly. (b) Corresponding diffraction pattern, where the inset shows an enlarged image of the (222) reflection from the $[\bar{2}11]$ zone indicated by the square. (c) Observation of the bubble superlattice in an adjacent grain at the same position. Here, the orientation is such that individual bubbles can be more clearly observed.

found in naturally-occurring radioactive minerals and is called metamictisation. Amorphisation is expected to lead to the undesired break-away swelling behaviour seen in irradiated U_3Si or U_6Fe-based dispersion fuel plates [11,14,15], because these materials exhibit a large increase in free volume by the amorphisation. Although U_3Si_2 is also said to become amorphous under irradiation, the amorphisation of the compound is apparently not accompanied by a large increase in free volume, which keeps its viscosity high enough to present a stable fission gas bubble growth [16].

However, analyses of irradiated U(Mo) from pin-type elements with neutron diffraction [17] have revealed the presence of well-crystallised UAl_3-type structures, which is the expected structure of the interaction phase in view of its composition [6].

The observations of the interaction layer formed in the FUTURE fuel as reported in this paper demonstrate the completely amorphous nature of this layer. The diffraction pattern shows a scatter disc with no indication of short-range order. However, the observation that the layer is completely amorphous in this sample, does not necessarily mean that no UAl_x-type structures are formed in other irradiation conditions. Indeed, a relation between fuel temperature, Al content of the interaction phase and the amorphisation is known to exist [18] and explains why UAl_3-type structures were found in the pin type fuel analysed in [17], since pin type fuel is generally operated at higher temperatures, which can cause recrystallisation of the interaction phase.

It will be interesting to compare the average nearest neighbour distance of 0.239 nm found in this sample with values obtained on other samples in which additives to the matrix or the fuel have been used to impede formation of the interaction phase or to improve its properties. The average nearest neighbour distance has a direct relation with the diffusion properties of a metallic glass, which in turn have their bearing on the mobility of gas bubbles in this material.

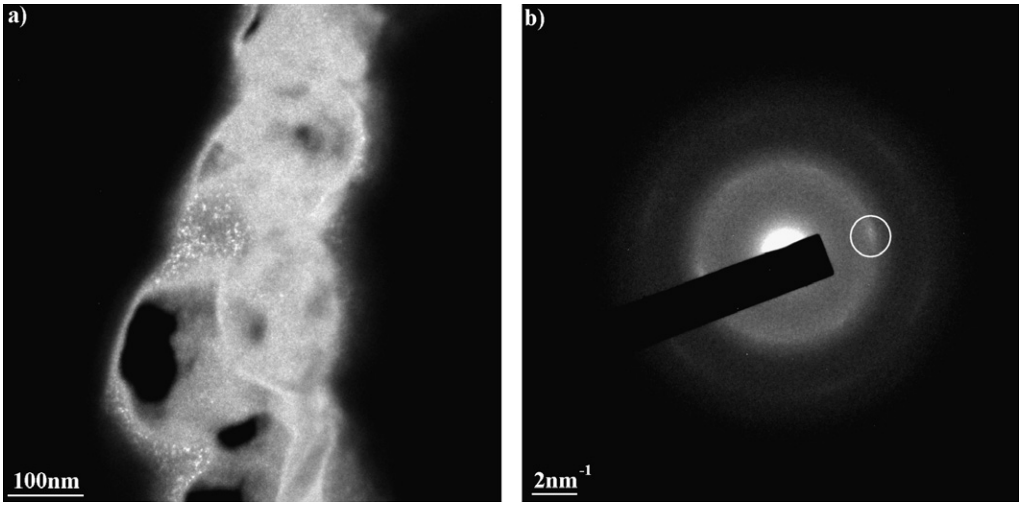

Fig. 5. (a) Dark-field image and (b) diffraction pattern of the U(Mo) phase on the cell boundaries in the U(Mo) atomised particles, found at position 4 as indicated in Fig. 1. The majority of the phase appears to be amorphous and the grainy contrast observed at some locations is related to the presence of oxide particles. In the diffraction pattern (b), the white circle indicates the chosen position of the objective aperture, at the location of the slightly more elevated diffracted intensity.

Not only the interaction layer, but also the layer between the cells of the U(Mo) atomised particles shows this amorphous nature. For the latter layers, however, the sample preparation may interfere with a fully conclusive observation, but the PIE results in [6] report the formation of bubbles in these cell boundaries, which could also point to poor gas retention caused by local amorphisation.

The U(Mo) itself has remained crystalline and shows sharp reflections in the diffraction pattern. Oxidation of the U(Mo) has taken place during sample preparation and storage forming small UO_2 particles, which is visible as diffraction rings with spacings that are typical for UO_2. Although generally randomly oriented, there is a preferred orientation for the UO_2 particles, as expected for oxide formation on a single crystal surface. The preferred orientation is derived from the more important diffracted intensity close to the U(Mo) diffraction spots (Fig. 3(c)). Dark-field images of the U(Mo) cells recorded using a U(Mo) diffraction spot (Fig. 3(b)) show a picture that highly resembles the dark-field images made using part of the UO_2 diffraction ring (Fig. 3(a)). Since a contribution of the UO_2 ring cannot be avoided in the dark-field image of the U(Mo) because of the size of the aperture, it is expected that the image contrast is caused by the UO_2 particles rather than that small U(Mo) particles would have been formed. The contrast differences observed in the two dark-field images shown in Fig. 3 support this assumption.

At higher magnification, the U(Mo) particles also reveal the formation of an ordered superlattice of fission gas related nanosized bubbles (Fig. 4(a)). Formation of such gas bubble superlattices has been observed in many metals after implantation with He gas [19–22] at temperatures below 0.2 T_m where T_m is the melting temperature (in K) of the metal. No previous reports of the formation of such superlattices by fission gases have been found. In view of the irradiation temperature of about 320 K (150 °C) and the melting temperature of pure uranium of 1405 K (T_m for U(Mo) is not expected to deviate largely from this value), the conditions for formation of these lattices are nearly fulfilled. Taking into account the difference between Xe and He as implanted gas, it can be expected that slightly higher temperatures will still lead to the bubble lattice formation for the heavier Xe atoms. The bubbles have a size of around 2 nm and a lattice spacing of 6–7 nm is found, which indicates, based on a 3-dimensional regular lattice, an estimate for the concentration of approximately $3 \times 10^{24}\ m^{-3}$ and a volume fraction of 1.3%. The fission gas bubble superlattice in this study is found to be fully coherent with the crystal structure of γ-U(Mo) and give rise to satellite diffraction spots (inset of Fig. 4(b)).

It was considered that the features are in fact not gas-filled bubbles but clustered defects resulting from the neutron irradiation. Such void superlattices have been reported before in irradiated materials, but they generally have different aspects, with larger void spacings. They are also expected to form only at temperatures above one third of the melting temperature (in K), where vacancies have sufficient mobility to cluster [21].

To model their recent Small Angle Neutron Scattering (SANS) data on irradiated U(Mo) fuel, Golosov et al. [23] introduce a monodispersed population of particles of 2 nm size (assumed to be UAl_3 type structures). Furthermore, a scattering peak at a wave vector q of 0.8 nm^{-1} is observed, which is explained using Guinier-Preston (GP) zones, but which can be interpreted as a diffraction peak caused by the superstructure with its 6–7 nm d-spacing. Both aspects of the SANS data are therefore in very good agreement with the bubble structure observed in our work.

The formation of these 3-dimensionally ordered bubble lattices could have a technological consequence as well, since this superlattice stage is generally reported to be followed by the formation of highly swollen nanoporous structures in other metals, but only at higher gas concentrations [22]. Also for the modelling of swelling and bubble development and behaviour in research reactor plate fuels [24], an accurate description of the way in which fission gas is accommodated in these fuels is required.

The amorphous interaction phase is not a good host for the bubble superlattice, and the reaction between the pure Al matrix and the U(Mo) particles will lead to the coalescence of the stored gas into large porosities, as observed in the FUTURE post-irradiation examinations [6]. Furthermore, the additionally formed fission gas in the glassy interaction product will have a high mobility and will migrate towards the porosities, causing further swelling.

5. Conclusion

The transmission electron microscopy investigation of a sample of irradiated U-7 wt% Mo atomised dispersion fuel extracted from the experimental fuel plates of the FUTURE experiment has confirmed the suspected amorphisation of the U(Mo)–Al interaction layer. This observation is the first direct proof of the transformation of the interaction phase, generally regarded as the most probable cause for the breakaway swelling observed.

It has furthermore revealed that a superlattice of fission gas bubbles has formed in the U(Mo) alloy itself. The superlattice is found to be fully coherent with the U(Mo) host lattice. The glassy U(Mo)–Al interaction layer will not support the bubble lattice, which will cause the bubbles to coalesce and lead to the development of large cavities, as was observed in the post-irradiation examinations of the FUTURE fuel and of most other U(Mo)-based irradiated fuel plates.

Acknowledgements

The authors would like to thank P. Lemoine and S. Dubois from CEA for the use of their fuel. The authors are also indebted to D. Sears and his AECL colleagues for their advice on sample preparation.

References

[1] A. Leenaers, E. Koonen, P. Lemoine, S. Van den Berghe, J. Nucl. Mater. 375 (2008) 243.

[2] E. Hélaine, P. Bernard, D. Leach, J.L. Emin, F. Gouyaud, in: Proceedings of the 10th International Topical Meeting on Research Reactor Fuel Management (RRFM), Sofia, Bulgaria, 2006.

[3] S.C. Parida, S. Dash, Z. Singh, R. Prasad, V. Venugopal, J. Phys. Chem. Sol. 62 (2001) 585.

[4] S.L. Hayes, M.K. Meyer, G.L. Hofman, R.V. Strain, in: Proceedings of the 21st International Meeting on Reduced Enrichment for Research and Test Reactors (RERTR), São Paulo, Brazil, 1998.

[5] A. Languille, J.P. Durand, A. Gay, in: Proceedings of the 3rd International Topical Meeting on Research Reactor Fuel Management (RRFM), Bruges, Belgium, 1999.

[6] A. Leenaers, S. Van den Berghe, E. Koonen, C. Jarousse, F. Huet, M. Trotabas, M. Boyard, S. Guillot, L. Sannen, M. Verwerft, J. Nucl. Mater. 335 (2004) 39.

[7] A. Leenaers, S. Van den Berghe, E. Koonen, C. Jarousse, F. Huet, M. Trotabas, M. Boyard, S. Guillot, L. Sannen, M. Verwerft, in: Proceedings of the 8th International Topical Meeting on Research Reactor Fuel Management (RRFM), Munich, Germany, 2004.

[8] D.F. Sears, Personal communication: TEM preparation electrolyte, 2006.

[9] A.E. Dwight, J. Nucl. Mater. 2 (1960) 81.

[10] P. Lemoine, J.L. Snelgrove, N. Arkhangelsky, L. Alvarez, in: Proceedings of the 8th International Topical Meeting on Research Reactor Fuel Management (RRFM), Munich, Germany, 2004.

[11] G.L. Hofman, Y.S. Kim, M.R. Finlay, J.L. Snelgrove, S.L. Hayes, M.K. Meyer, C.R. Clark, F. Huet, in: Proceedings of the 25th International Meeting on Reduced Enrichment for Research and Test Reactors (RERTR), Chicago, Illinois, 2003.

[12] G.L. Hofman, M.R. Finlay, Y.S. Kim, in: Proceedings of the 26th International Meeting on Reduced Enrichment for Research and Test Reactors (RERTR), Vienna, Austria, 2004.

[13] G.L. Hofman, Y.S. Kim, H.J. Ryu, J. Rest, D.M. Wachs, M.R. Finlay, in: Proceedings of the 10th International Topical Meeting on Research Reactor Fuel Management (RRFM), Sofia, Bulgaria, 2006.

[14] M.R. Finlay, G.L. Hofman, J.L. Snelgrove, J. Nucl. Mater. 325 (2004) 118.

[15] G.L. Hofman, L.A. Neimark, in: Proceedings of the 10th International Meeting on Reduced Enrichment for Research and Test Reactors (RERTR), Buenos Aires (Argentina), 1987.

[16] G.L. Hofman, Y.S. Kim, Nucl. Eng. Technol. 37 (2005) 299.

[17] K.T. Conlon, D.F. Sears, in: Proceedings of the 10th International Topical Meeting on Research Reactor Fuel Management (RRFM), Sofia, Bulgaria, 2006.

[18] H.J. Ryu, Y.S. Kim, G.L. Hofman, D.D. Keiser, in: Proceedings of the 28th International Meeting on Reduced Enrichment for Research and Test Reactors (RERTR), Cape Town, South Africa, 2006.

[19] Gas Bubble Lattices in Metals, in: S.E. Donnely, J.H. Evans (Eds.), Fundamental Aspects of Inert Gases in Solids, Plenum, NY, 1991.

[20] P.B. Johnson, F. Lawson, Nucl. Instrum. Methods Phys. Res. B 243 (2006) 325.

[21] V.I. Dubinko, A.A. Turkin, Appl. Phys. A 58 (1994) 21.

[22] P.B. Johnson, R.W. Thomson, K. Reader, J. Nucl. Mater. 273 (1999) 117.

[23] O.A. Golosov, V.B. Semerikov, S.G. Bogdanov, M.S. Lyutikova, in: Proceedings of the 29th International Meeting on Reduced Enrichment for Research and Test Reactors (RERTR), Prague, Czech Republic, 2007.

[24] J. Rest, G.L. Hofman, I.I. Konovalov, A.A. Maslov, A.A. Bochvar, in: Proceedings of the 21st International Meeting on Reduced Enrichment for Research and Test Reactors (RERTR), São Paulo, Brazil, 1998.